

Accuracy evaluation and verification of FISP sediment samplers through CFD modeling

Project report to U.S. Geological Survey
under Cooperative Agreement G15AC00193

Prepared by

Xiaofeng Liu, Ph.D., P.E., Assistant Professor
Yuncheng Xu, Graduate Research Assistant

Department of Civil and Environmental Engineering
Pennsylvania State University
Contact Email: xliu@engr.psu.edu
Web: <http://water.engr.psu.edu/liu>

June, 2016

Executive Summary

The purpose of this project was to use the state-of-art 3D computational fluid dynamics (CFD) model to evaluate and verify the accuracy of FISP sediment samplers. Turbulent open channel flow and suspended sediment were simulated around two selected depth-integrating samplers, D95 and D96. The intrusion effect of the samplers and their accuracy were studied. Past investigations have mostly used laboratory experiments or field measurements. Though they resulted in abundant useful information, the detailed 3D flow and suspended sediment distributions with the presence of the samplers, in comparison with the undisturbed conditions, are not clear. This lack of details is the major source of uncertainty in the measuring results. The CFD modeling work helps reduce the uncertainty and improve the measurement accuracy. The CFD package used in this project was the open source platform OpenFOAM. Suspended sediment transport module was implemented to simulate the entrainment, transport and deposition processes. The turbulence was simulated using a Reynolds-Averaged-Navier-Stokes (RANS) $k-\omega$ model. In the simulations, the samplers were placed at three different vertical locations in an open channel. The simulation results show that the surrounding flow is disturbed by the sediment samplers. However, regardless the vertical location of the samplers, they have negligible disturbance on the sediment concentration at the nozzle inlet. The main reason is that the inlet nozzle of both samplers has enough protrusion upstream such that the intake is not affected by the sampler bodies. The results did not show significant vorticity at the inlet nozzle, which in the past has been suspected to impart centrifugal force on sediment particles and thus have selective sampling efficiency depending on sediment sizes.

This research is limited in the following aspects and future research should consider improvement accordingly. The velocity at the inlet nozzle was fixed and the inflation process of the plastic bag within the sampler was not modelled. Therefore, the inflow speed variation was not considered. A simple solution would be to perform an equivalent flume test and record the inflow rate to be used as inlet condition. Secondly, the “flight path” effect was not considered. At the descending and ascending phases of the sampling process, the drift angle will change. We anticipate that during the ascending phase, the disturbance (vortices shed from the sampler body) will prorogate to the inlet and thus disturb the sampling accuracy. Third, only RANS simulations was performed. If the eddies are resolved using large eddy simulation (LES), the instantaneous swirl might show at the nozzle and the sediment particle response to the swirl can be simulated.

1 Introductions

Suspended sediment concentration in rivers and streams is important for both engineering and scientific communities. A representative value of suspended sediment concentration at a river cross section is the depth-averaged concentration. There are three major types of depth-averaged suspended sediment samplers, namely rigid-bottle depth-integrating sampler, collapsible-bag depth-integrating sampler, and point-integrating sampler. The depth-integrating suspended sediment samplers have been widely used in the field. A depth-integrating sampler intakes sediment-laden flow during its downward movement from water surface to the river bottom and upward movement back to the water surface. The sediment concentration in the filled sampler will be used to represent the depth-integrating value. A key question is the accuracy of the measured concentration in comparison with the true value. There have been speculations that the intrusive nature of the samplers will disturb the flow and thus reduce the accuracy.

In the past, several flume and field investigations have been conducted on different types of sediment samplers, which studied the inflow efficiency, operating velocity, transient rate, bag filling time, drift angle and so forth. These studies helped determine the operating range of the ambient velocity as well as the maximum water depth for different types of samplers with nozzles of different diameters. However, there has no direct research on the suspended sediment disturbance due to the measurement difficulty in experiments. Ideally, for a suspended sediment sampler to work perfectly, there are several important design criteria:

- to allow a water-sediment mixture to enter the nozzle isokinetically,
- to permit the sampler nozzle to reach a point as close to the stream bed as physically possible
- and to minimize disturbance to the flow pattern of the stream, especially at the nozzle.

This project aims to use computational fluid dynamics (CFD) simulations to address the third criterion, i.e., to quantify the effects of sampler intrusion on the local flow and sediment transport, thus the measurement accuracy.

Two hypotheses are proposed and tested in this project:

- H1: Flow is disturbed by the sampler and therefore the measured sediment concentration deviates from its undisturbed value.
- H2: Inlet flow through the nozzle has vorticity such that sediment particle could be “swept” out of the flow due to centrifugal force and thus bias the concentration result.

The rest of this report is organized as follows. First, the modeling framework and process are described, which include the preparation of sampler geometries, CFD model, and simulation conditions. Then the simulation results are presented and discussed. This report ends with the conclusions and future research suggestions.

2 Modeling framework

2.1 Geometry preparation

In this project, two types of suspended sediment sampler, D95 and D96, were selected. Their 3D geometries were constructed from the drawings provided by USGS (McGregor, 2000; Davis, 2001). The construction was processed in the open source software FreeCAD, as shown in Fig. 1.

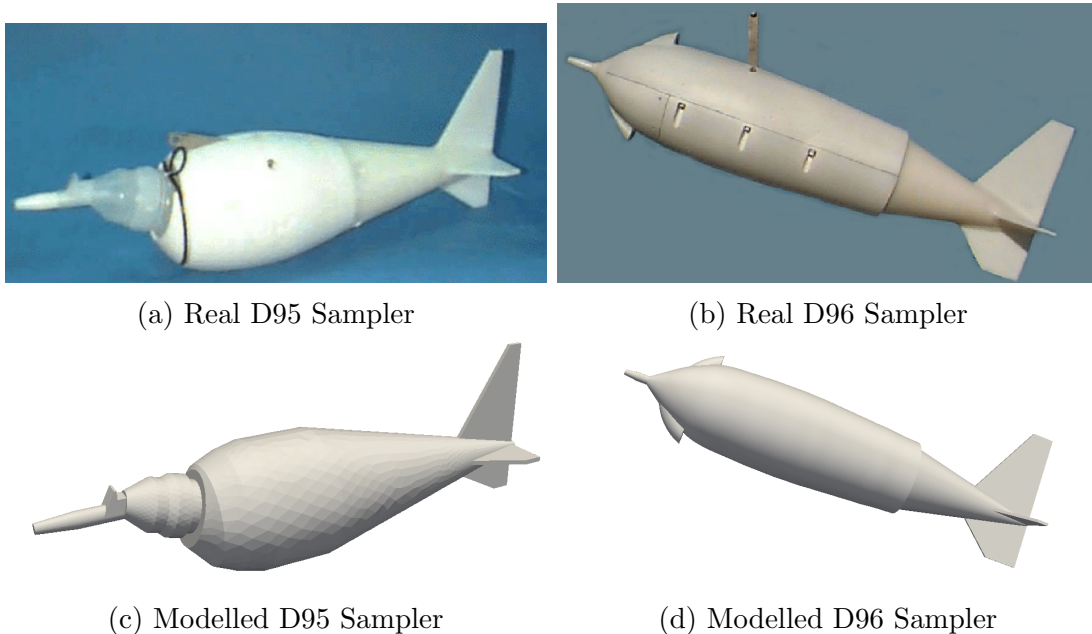


Figure 1: The images and constructed 3D models of D95 and D96 samplers.

From the comparison between the real images and the constructed 3D geometries of the samplers in Fig. 1, one can observe that some simplifications were made during the geometry preparation:

- only the external geometry is considered,
- small features such as the stamped text and the drilling holes are ignored.

These simplifications are anticipated not to have great impact on the final results because the features ignored are rather insignificant.

2.2 Computational model

The open source CFD platform OpenFOAM[®] was used in this project. Since its debut in the open source community, OpenFOAM[®] user base from both academia and industry has expanded tremendously. The application areas are rather extensive and span a wide spectrum in engineering and sciences. OpenFOAM[®] is designed to capture complex flow features with a wide range of models for turbulence.

The state-of-art 3D computational fluid dynamics (CFD) in OpenFOAM[®] was performed

to evaluate and verify the accuracy of FISP sediment samplers. The simulation of the turbulent open channel flow is governed by Reynolds-averaged Navier-Stokes (RANS) equations. A $k-\omega$ RANS model was used (Wilcox, 2006). The suspended sediment field was simulated by a sediment solver which was developed by the authors (Liu, 2014), where suspended sediment transport module was added to OpenFOAM[®], with the governing equation as follows:

$$\frac{\partial C}{\partial t} + \nabla \cdot [(\mathbf{u} + \mathbf{w}_s)C] = \nabla \cdot (\epsilon_s \nabla C) \quad (1)$$

where C is the volumetric suspended sediment concentration, \mathbf{u} is the flow velocity, \mathbf{w}_s is the sediment settling velocity, ϵ_s is the sediment diffusivity ($= \nu_t / \sigma_c$), ν_t is the turbulent eddy viscosity calculated from the turbulence model, and σ_c is the Schmidt number which had a value of 1 in this model.

To simulate the samplers in the computational model, proper meshes were generated based on the 3D geometries. OpenFOAM[®] has a very efficient tool named *snappyHexMesh* to generate the mesh for complex geometries such as the sediment sampler. The procedure of mesh generation was:

- Use *blockMesh* to create background mesh, as shown in Fig. 2. *blockMesh* is another tool to build relatively simple meshes which can be used as foundations for more complex ones.

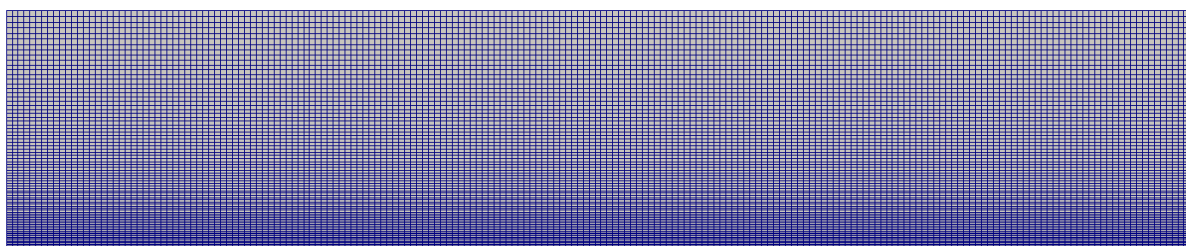


Figure 2: Background mesh built by *blockMesh*. The mesh is shown in 2D. But the real mesh is 3D.

- Use *snappyHexMesh* to create the mesh due to the introduction of the sampler, as shown in Fig. 3. In this figure, the D95 mesh is shown as an example.

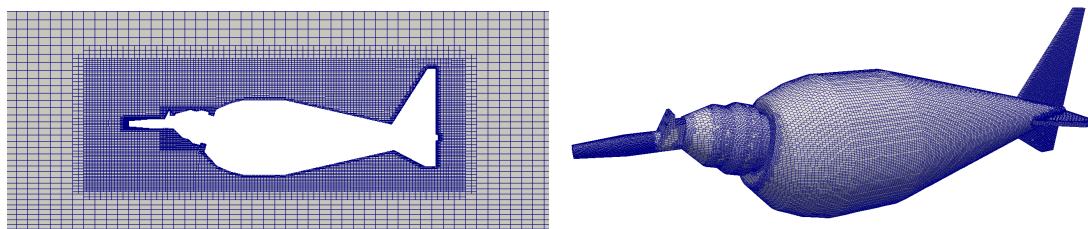


Figure 3: Mesh with the sampler D95

It can be seen in the mesh, the region near the nozzle and around the body is refined to capture more details in this area of interest. The total number of cells is 2.3-3.3 million for the mesh with the D95 sampler, and 2.7-4.0 million for the mesh with the D96 sampler. The range of cell numbers reflects the test in the simulations for mesh independence. The finer resolution was used at the end. The grid size for the background case mesh was

about 1.25-2.5 cm. There were four different refinement levels, which means the most refined grid size can be as small as 1.25×2^{-4} cm \approx 0.78 mm. The region near the inlet nozzle used the 4th refinement level, while the region near the sampler body uses the 3rd refinement level.

2.3 Conditions for flow and sediment

The flow condition was set up based on the recommended operational flow ranges for the samplers. Fig. 4 shows the experimental data on inflow efficiency, which is the ratio of the nozzle intake velocity and the ambient velocity, for the 1/4 inch nozzle of the D95 sampler. The recommended operating range of the ambient velocity is determined with 10% error, which is between 0.5 m/s and 2 m/s. The D96 sampler has a similar range. Thus, in this project we selected mean velocity of 1.5 m/s as the representative ambient velocity in the channel.

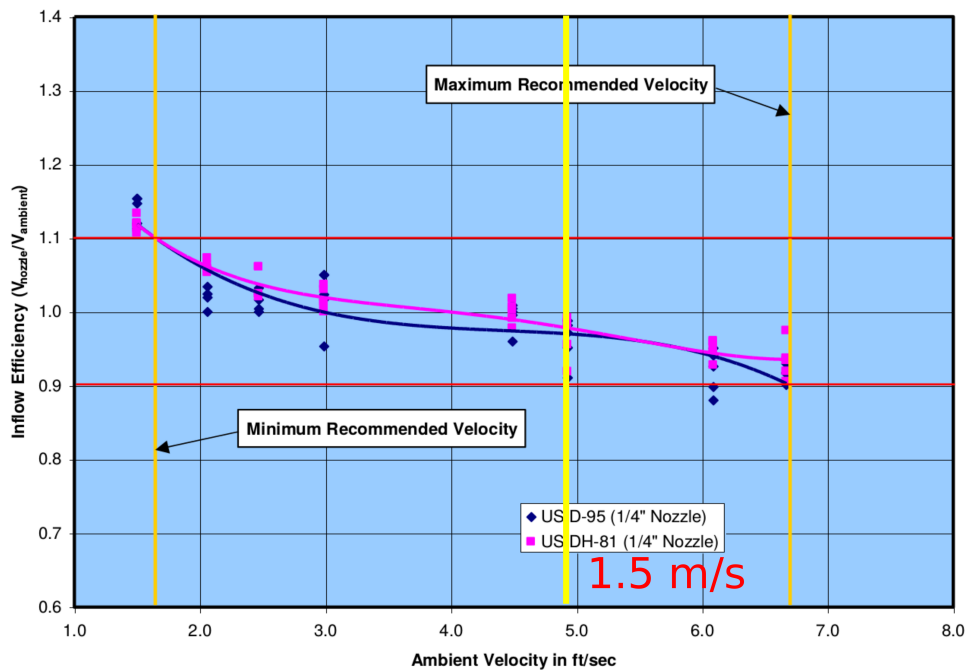


Figure 4: Inflow efficiency for the 1/4 inch nozzle, from Report LL, Development of the US D-95 Suspended-Sediment Sampler (McGregor, 2000).

The scheme of the channel and the relative location of the sampler are shown in Fig. 5. Based on previous flume experiments, the simulated channel was designed with a height of 1 m, a width of 2 m and a length of 5 m. In order to model the effect of sampler location during the measurement process, three vertical positions were chosen. The vertical location was noted based on the nozzle tip elevation:

- A: upper, close to the free surface, 0.8 m from the bottom
- B: middle, 0.5 m from the bottom
- C: lower, 0.2 m from the bottom

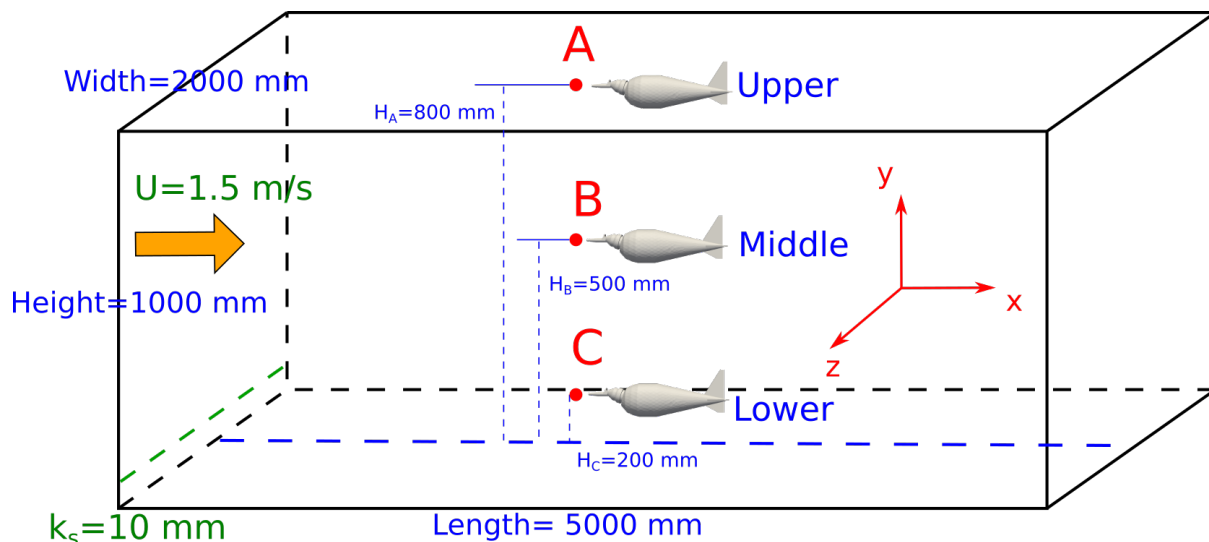


Figure 5: Schematic view of flow conditions and sampler locations.

In addition, the simulated channel had a rough bottom with roughness height of 10 mm to mimic the rough bottom conditions often encountered in the field. And the sediment size on the bottom is set as $D_{50} = 150 \mu\text{m}$ and $D_{50} = 300 \mu\text{m}$.

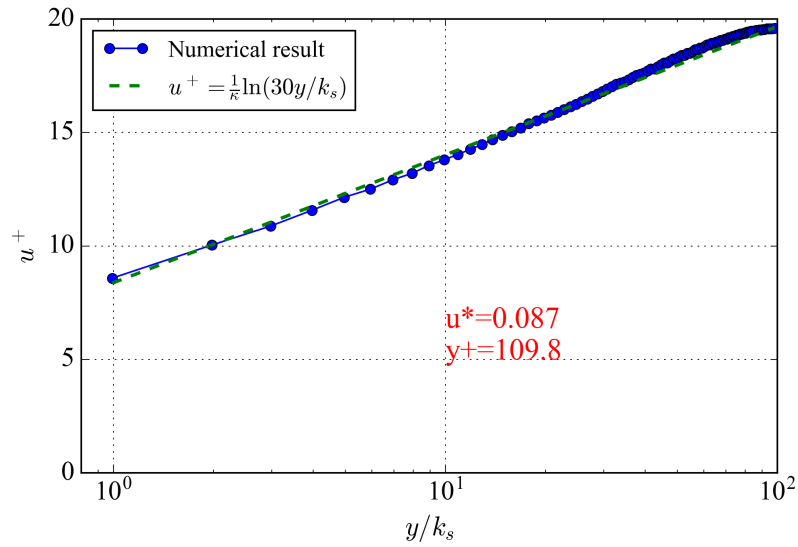
3 Simulation Results

3.1 Background flow field without sampler

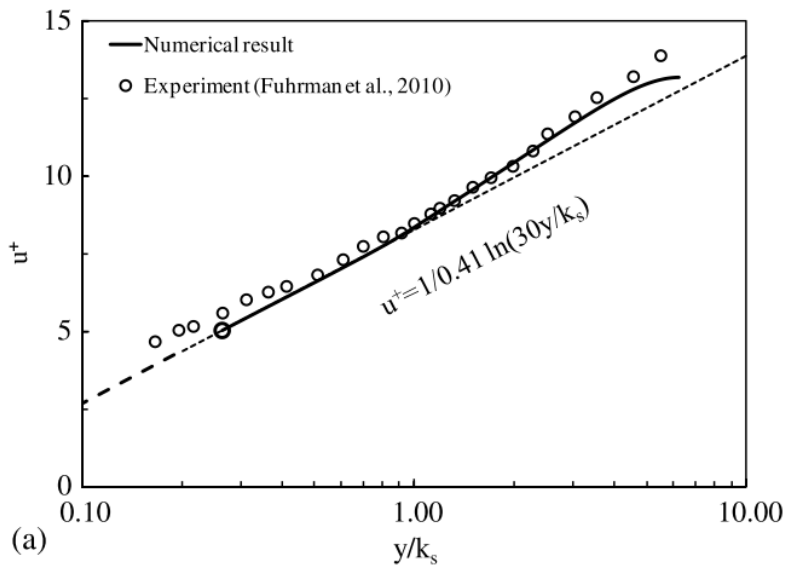
For comparison, the background flow and suspended sediment concentration fields without the samplers were simulated first. In Fig. 6, the computed average background velocity profile is plotted using the logarithmic scale, compared with the results in Liu (2014). The simulated velocity generally follows the log-law for turbulent flow over rough walls. For the bottom wall boundary, a wall function was used. To accommodate this in the the CFD model, the near-wall grid size needs to be in the log-law layer. Generally, the dimensionless grid size y^+ in wall unit should be larger than 25 and smaller than 200. In this research, y^+ was about 110 which was in the proper range.

For the background simulation case, at steady state, the settling flux of sediment in the vertical direction is balanced by turbulent suspension. The turbulent suspension can be modeled through the turbulent eddy viscosity. Fig. 7 shows the averaged background vertical distribution of turbulent eddy viscosity, in comparison with the simulation results and experimental data reported in Liu (2014). In the current setup, the eddy viscosity follows a parabolic-constant distribution, which has been observed in many laboratory and field measurements.

The steady state suspended sediment concentration profiles are plotted in Fig. 8, which generally follow the Rouse profile. In these figures, the Rouse parameter Z is defined as $w_s/(\kappa u_*)$ and C_{b*} is the reference concentration at a reference height.

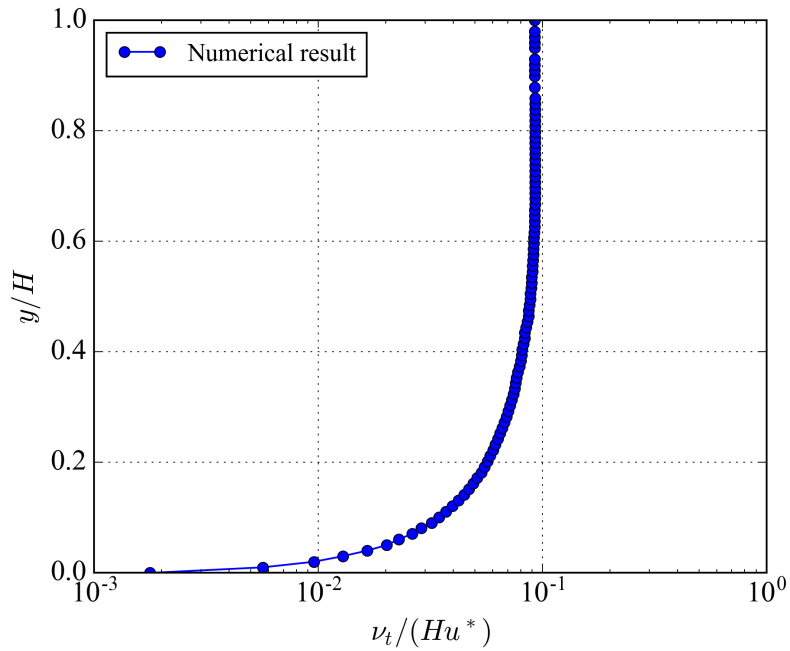


(a) Present study $y^+ = 109.8$

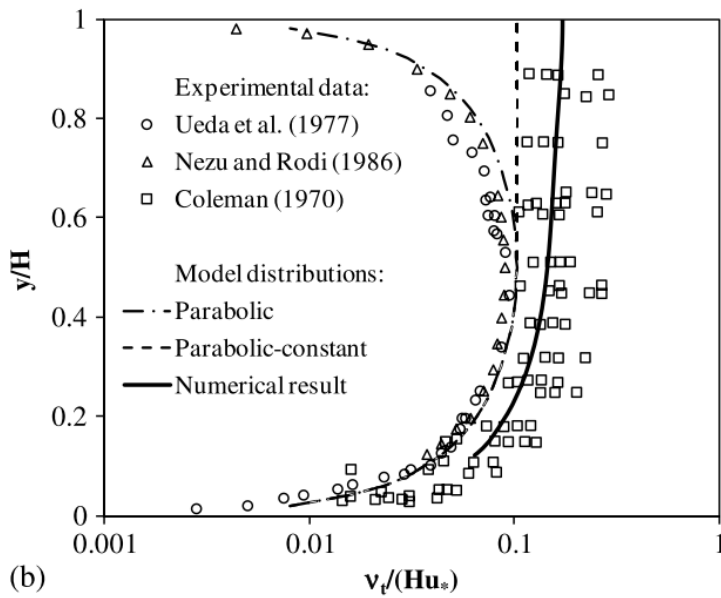


(b) Liu (2014), $y^+ = 52.5$

Figure 6: Average background vertical velocity distribution: (a) velocity distribution in this research, (b) velocity distribution in Liu (2014).

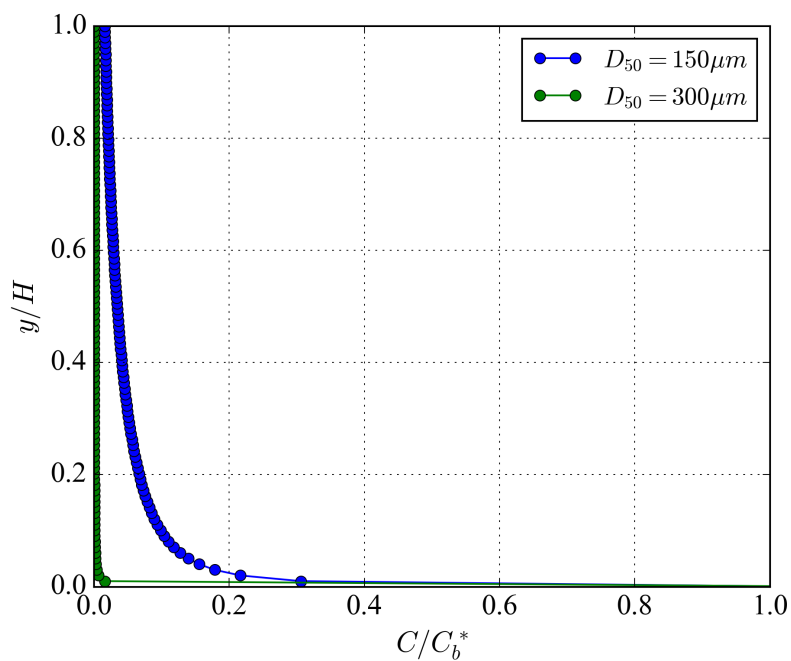


(a) Present study $y^+ = 109.8$

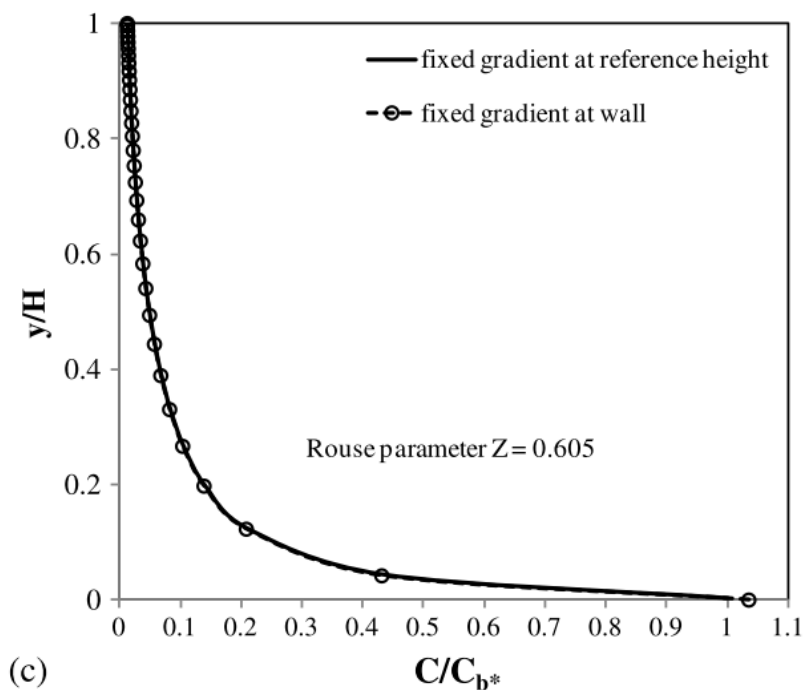


(b) Liu (2014), $y^+ = 52.5$

Figure 7: Averaged background vertical distribution of turbulent viscosity



(a) Present study, Rouse parameter $Z = 0.438$ for $D_{50} = 150 \mu m$ and $Z = 1.168$ for $D_{50} = 300 \mu m$



(b) Liu (2014), Rouse parameter $Z = 0.605$ for $D_{50} = 79 \mu m$

Figure 8: Averaged background vertical distribution of sediment concentration

3.2 Flow field with samplers

Due to the introduction of the samplers, the flow field is disturbed. As an example shown in Fig. 9, the streamlines around the D95 sampler obviously show that the flow is disturbed by the sampler.

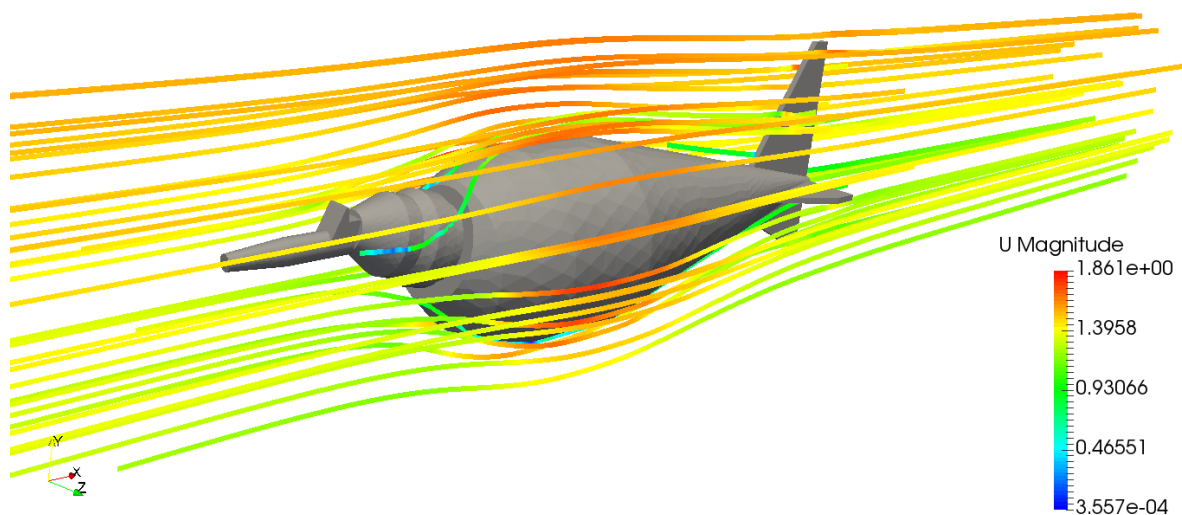


Figure 9: Streamlines around the D95 sampler

Fig. 10 shows the velocity magnitude distribution on the center slice with the existence of D95 sampler. It can be seen that for all the three sampler vertical positions, the velocity gets higher on the up and down sides of the sampler due to the squeeze on the flow. The wake in the downstream side of the sampler can also be clearly observed in both the upper and middle positions. For the lower position, the zoom-in view is shown in Fig. 11 for better visualization. With different color map, the effect of the sampler is easy to be recognized. The disturbance due to the small features on the sampler head can be also observed. However, from these contour plots it is hard to distinguish whether the flow field changes significantly around the nozzle tip. Another way to visualize the impact on velocity is plotted in Fig. 12 for the cross-sectional distribution of velocity at the inlet nozzle tip. It shows that the velocity distribution has a slight decrease in the center near the nozzle.

Fig. 13 plots the vertical distribution of streamwise velocity u_x at the centerline with the D95 and D96 samplers. The deviation of velocity from the background case at the three positions appear to be different between D95 and D96 sampler. It shows D96 has a bigger disturbance than D95. In the simulations, the inlet velocity into the nozzle was fixed. However, in reality the inlet velocity at the nozzle is controlled by the pressure difference between the internal space of the sampler and the outside flow field. Since only the external geometry is considered in this model, this pressure difference can not be resolved and thus only a fixed inlet velocity was used.

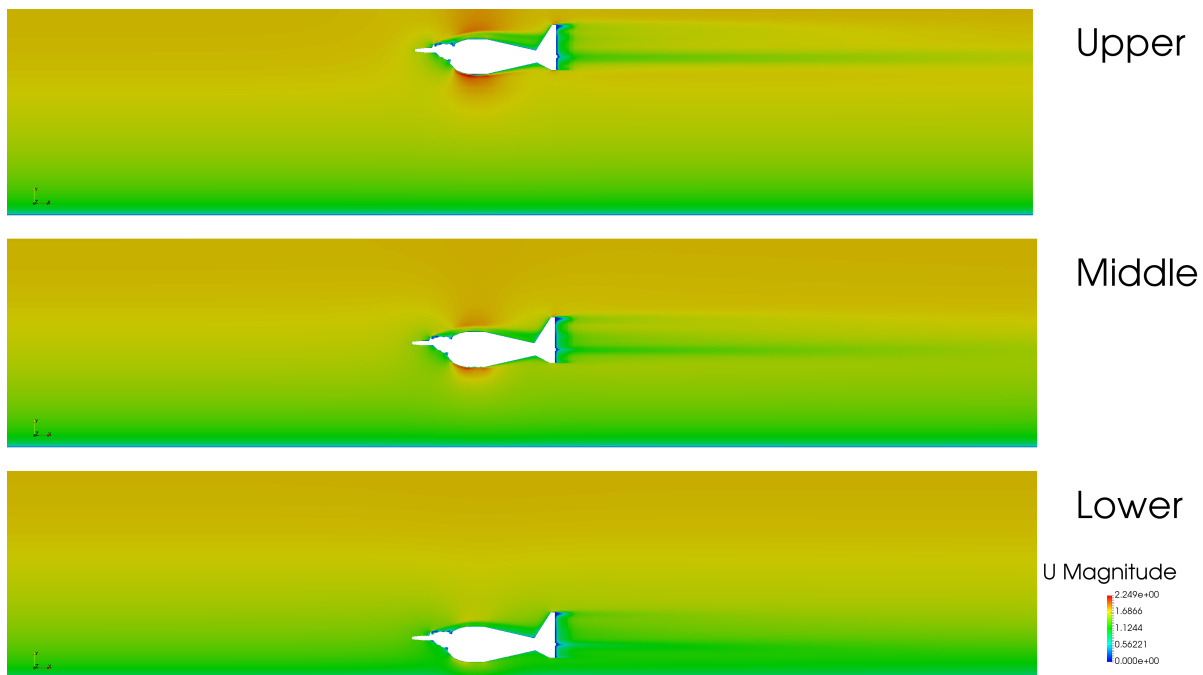


Figure 10: Velocity distribution on the center slice for the D95 sampler

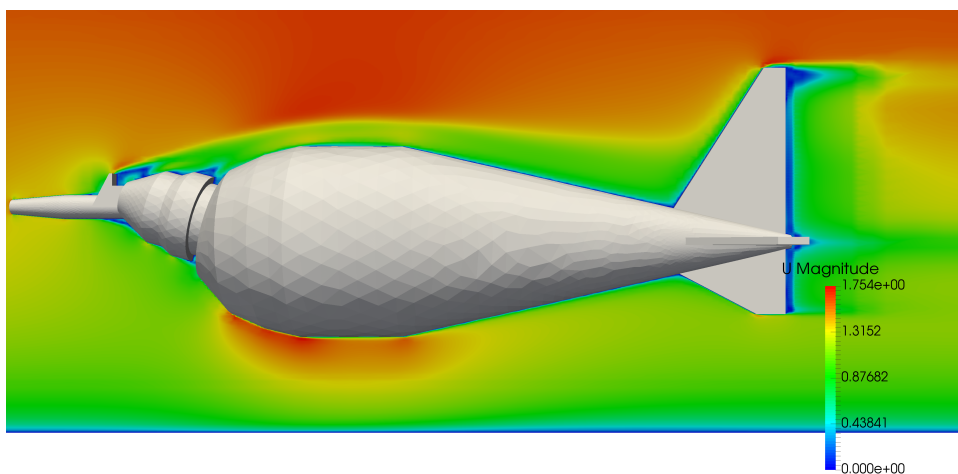


Figure 11: Zoom in view of velocity distribution for the lower position case for the D95 sampler

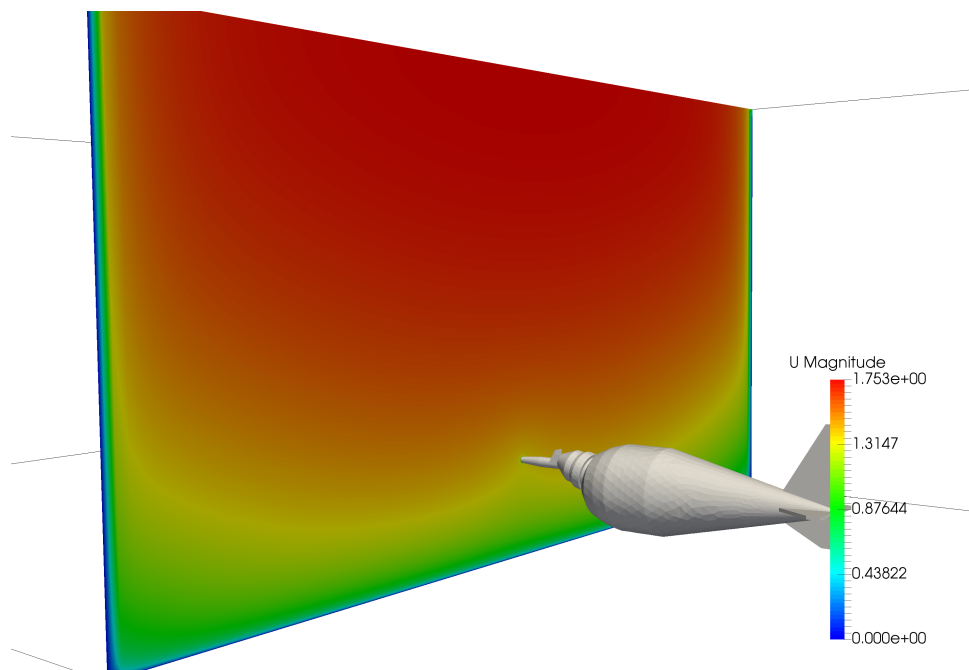


Figure 12: Velocity distribution on a cross-section at the inlet nozzle for the D95 sampler

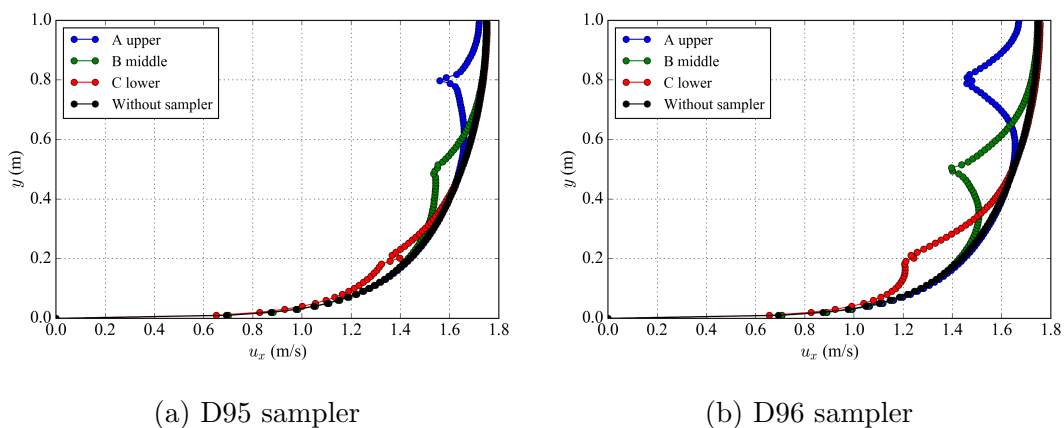


Figure 13: Vertical distribution of streamwise velocity u_x at the centerline

3.3 Sediment concentration distribution

The more important result is the suspended sediment intake. As seen in Fig. 8(a), the Rouse number in the background flow condition is 0.438 for $D_{50} = 150 \mu m$ and 1.168 for $D_{50} = 300 \mu m$. Fig. 14 shows the sediment concentration distribution with the D95 sampler at three different vertical locations. In general, for both the upper and middle vertical locations, the sediment concentration distribution does not change too much, partially due to the fact that most of the suspended sediment is near the bottom. However, for the lower vertical location case, a slight change can be observed in the sediment concentration distribution. A zoom-in view of the sediment concentration for the lower location case can be seen in Fig. 15. It can be observed that the sampler squeezes the higher concentration zone right below the body. The sediment concentration near the upper surface of the sampler is also higher than the undisturbed background flow. It seems that the sediment concentration keeps unchanged (green color) in the region near the upstream part of the sampler. The effect in the wake area is not so obvious.

The primary goal of this research is to see if the intrusion of the sampler has any impact on the inflow sediment concentration. Fig. 16 shows the sediment concentration distribution on the cross-section right at the inlet nozzle tip. It can be seen that there is no significant change of sediment distribution due to the sampler. To further examine the impact, Fig. 17 plots the vertical distribution of the sediment concentration at the vertical line passing through the inlet nozzle for $D_{50} = 150 \mu m$. It shows that for all three vertical locations, the intake sediment concentration is not affected too much by the sampler. $D_{50} = 300 \mu m$ has a similar trend. Table 1 lists the relative change of the intake sediment concentration in comparison with the background case. It seems that the lower the sampler is located, the larger change there will be. And larger particle size seems have more change. However, all relative changes are less than 7%, which is trivial considering the uncertainties induced by other factors.

From the simulation results, it can be concluded that Hypothesis #1 is not true, which means the intake sediment concentration into the nozzle is almost undisturbed by the sampler. This is largely due to the protrusion of the nozzle into upstream and away from the body. On the other hand, the disturbance to the flow field and sediment transport around the sampler body is rather significant.

Table 1: Relative change of the intake sediment concentration between the cases with sampler and the background case.

	A Upper	B Middle	C Lower	
D95	0.07%	-0.07%	1.62%	$D_{50} = 150 \mu m$
D96	-0.29%	-0.37%	2.04%	
	A Upper	B Middle	C Lower	
D95	-0.7%	-1.15%	3.44%	$D_{50} = 300 \mu m$
D96	-2.11%	-1.90%	6.34%	

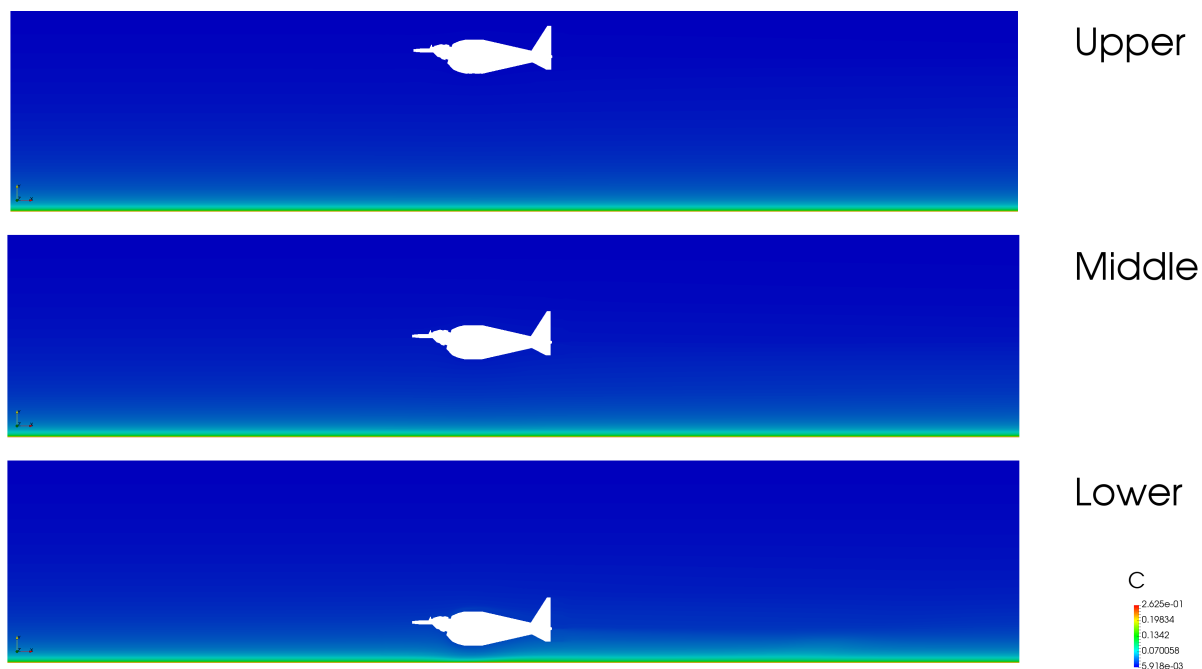


Figure 14: Contour of sediment concentration for the D95 sampler with $D_{50} = 150 \mu m$.

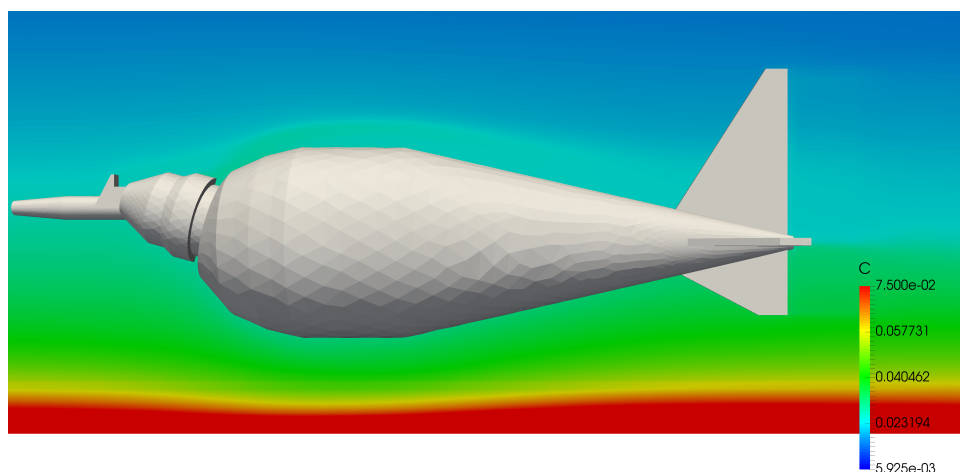


Figure 15: Zoom-in view of sediment concentration for the lower configuration for the D95 sampler with $D_{50} = 150 \mu m$.

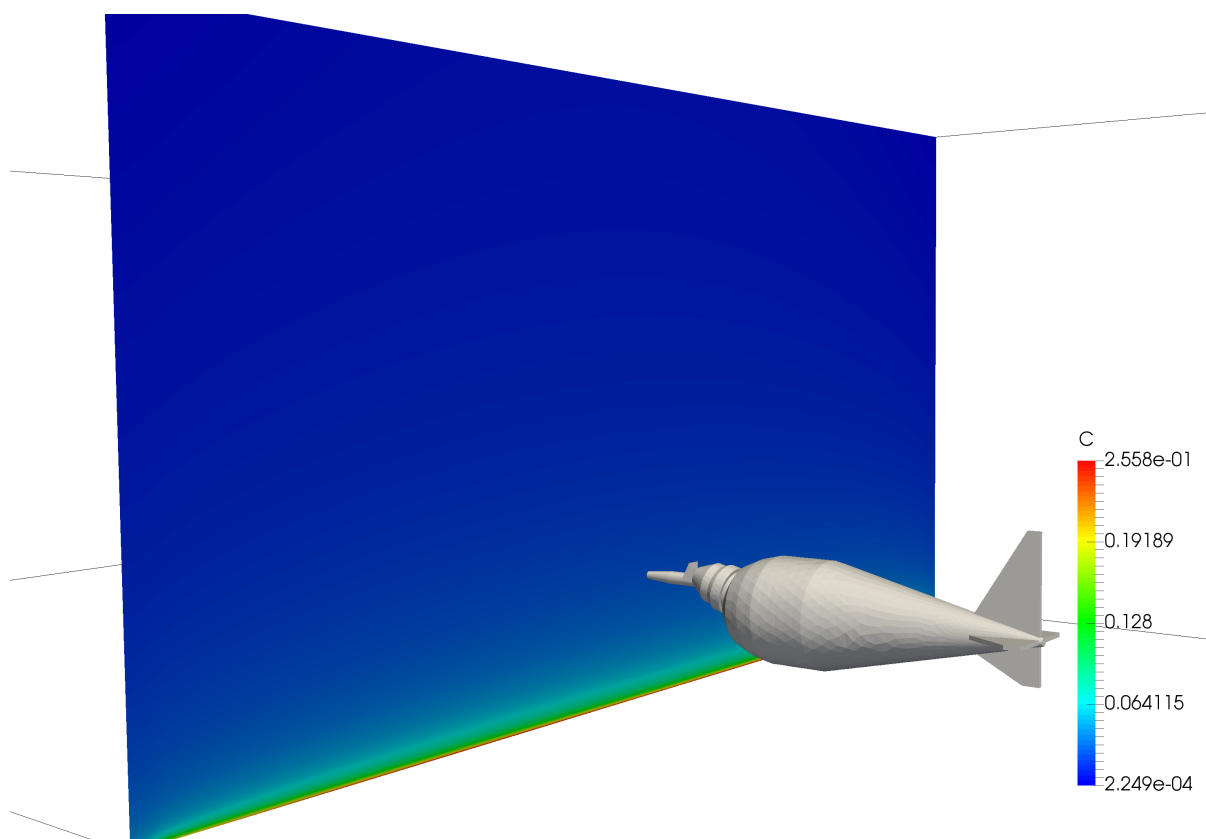


Figure 16: Sediment concentration on the cross-section at the inlet nozzle for D95 sampler with $D_{50} = 150 \mu m$.

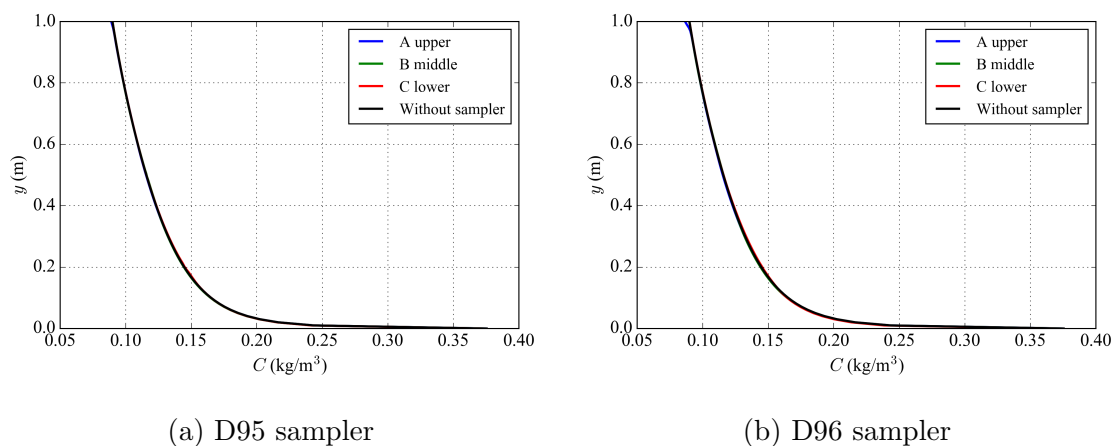


Figure 17: Vertical distribution of suspended sediment concentration at the inlet nozzle, for $D_{50} = 150 \mu m$.

3.4 Vorticity at inlet nozzle

Previously, it was speculated that there might be very strong vorticity near the small diameter nozzle, which might sweep the sediment particle out of the flow due to the centrifugal force. However, from the 2D and 3D contour of vorticity shown in Fig. 18 and Fig. 19, the vorticity contour near the inlet nozzle does not show any significant swirl for both samplers. Thus, the Hypothesis #2 on the swirl effect is not true either.

However, we want to note that there are some limitations on the RANS modeling approach. It can only give time-averaged flow field, which loses some important details of the instantaneous flow and eddies, especially near the inlet nozzle. Large eddy simulation (LES) would be a good tool to resolve the eddies, which is strongly recommended for further study.

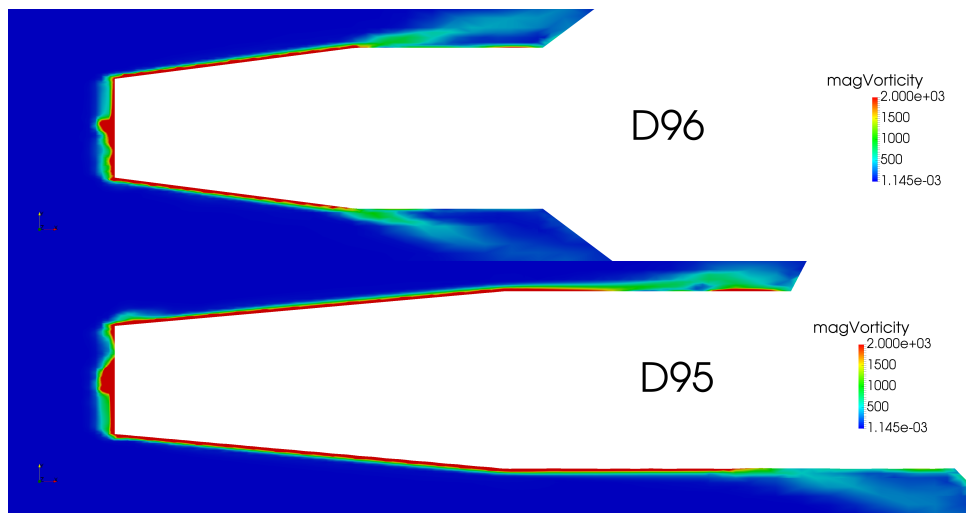


Figure 18: Distribution of vorticity magnitude around the inlet nozzle for D95 and D96 samplers.

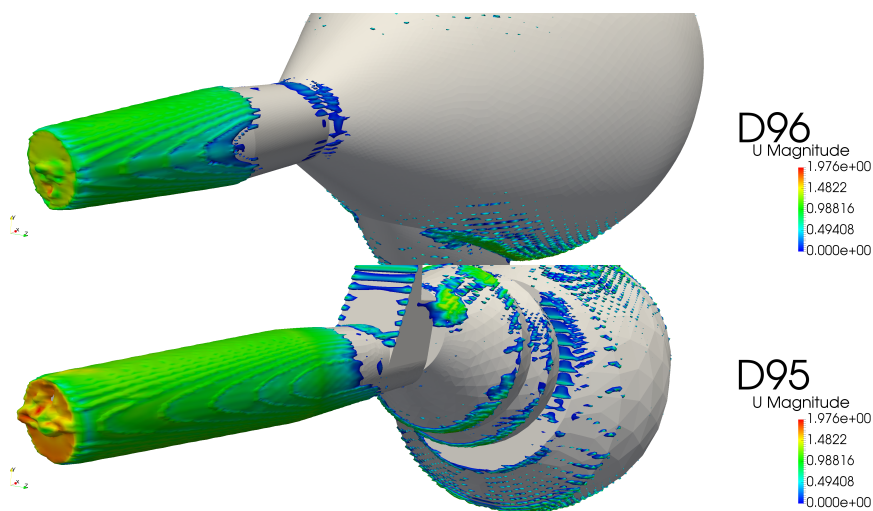


Figure 19: 3D contour of vorticity around the inlet nozzle for D95 and D96 samplers.

4 Conclusions

In this project, a 3D computational fluid dynamics (CFD) model implemented in OpenFOAM[®] was used to evaluate and verify the accuracy of two FISP depth-averaged suspended sediment samplers, namely D95 and D96. The turbulence was modeled using a RANS $k-\omega$ model. The suspended sediment transport module was also implemented. The numerical simulations were conducted in a 1 m high and 2 m wide channel. The samplers were placed at three different locations, namely upper, middle, and lower to simulate three representative conditions during the operation of the samplers.

The simulation results show that the surrounding flow is disturbed by the sediment samplers. However, regardless the vertical location of the samplers, they have negligible disturbance on the sediment concentration at the nozzle inlet. The main reason is that the inlet nozzle of both samplers has enough protrusion upstream such that the intake is not affected by the sampler bodies. The results did not show significant swirl at the inlet nozzle, which in the past has been suspected to impart centrifugal force on sediment particles and thus have selective sampling efficiency depending on sediment sizes.

There are some limitations in this research, which should be addressed in future research:

- Fixed velocity at the inlet nozzle:
 - The inflation of the plastic bag was not modelled. Thus the pressure difference between the outside and inside is unknown and the flow velocity into the inlet can not be calculated. Therefore, the inflow variation can not be resolved in this model. The inflow velocity had to be set as a fixed value according to the previous flume studies.
 - Suggestion: combine the modelling of the interior flow and the outside flow.
- “Flight path” effect not considered:
 - Due to the drift angle, the descending and ascending phases of the sampler are different. When the sampler is being lowered, the drift angle will become smaller due to the smaller drag force exerted on the sampler caused by the gradually decreasing velocity. On the other hand, when the sampler is being lifted, the drift angle will get larger.
 - Based on our results, we speculate that disturbance will propagate to inlet during the ascending phase.
- RANS simulations were performed. Only time-averaged flow field solutions were obtained. A future improvement would be to resolve eddies using large eddy simulation. With LES,
 - instantaneous swirl will show at the nozzle,
 - how sediment particles will respond to the instantaneous eddy (swirl) depends on its inertia. A combined LES and Lagrangian particle tracking modeling is recommended.

- In the simulations, the drag force exerted on the sampler can be calculated by integrating the pressure on the external surface, which can be seen in Table 2. Unfortunately, the gravity of the sampler is unknown. Otherwise, the drift angle can be estimated in this model.

Table 2: Drag force exerted on the samplers. x is the streamwise direction and y is the vertical direction.

type	position	U_x (m/s)	F_x (N)	F_y (N)
D95	Upper	1.73	3.88	0.44
D95	Middle	1.65	3.95	0.31
D95	Lower	1.44	3.69	0.83
D96	Upper	1.73	7.72	3.06
D96	Middle	1.65	7.41	0.97
D96	Lower	1.44	6.31	0.82

- Only flume test flow condition was used due to the absence of field data. This limits the water depth to 1 m. In reality, the water depth can be much larger.

5 Acknowledgement

The financial support of this research was provided by the USGS Federal Interagency Sedimentation Project through the Cooperative Agreement G15AC00193. We thank Dr. Mark Landers and other members of the FISP Technical Committee for their support and valuable comments on various aspects of this project.

References

- Davis, E. B. (2001). The US D-96: An Isokinetic Suspended-sediment/Water-quality Collapsible-bag Sampler. Technical report, U.S. Geological Survey.
- Liu, X. (2014). New Near-Wall Treatment for Suspended Sediment Transport Simulations with High Reynolds Number Turbulence Models. *Journal of Hydraulic Engineering* 140(3), 333–339.
- McGregor, J. (2000). Development of the US D-95 Suspended-sediment Sampler. Technical report, U.S. Army Corps of Engineers.
- Wilcox, D. (2006) Turbulence modeling for CFD. DCW Industries, Inc., La Candada CA.